

Supporting Information

Mechanically Robust Polyurethane Elastomers Enabled by Soft-Segment-Regulated Hydrogen Bonds and Microphase Separation for Ultrasound Imaging Medical Catheters

Yanlong Luo,^{a,b} Qingchuang Lu,^a Jianye Lu,^a Zuqian Chen,^c Chichao Li,^a Zhenyang Luo,^a Wu Cai,^c Chenghui-Li,^b Zhengdong Fei,^{*c} Qingbo Lu,^{*d} Yao Liu.^{*c}

^aCollege of Science, Nanjing Forestry University, Nanjing 210037, China

^bState Key Laboratory of Coordination Chemistry, Nanjing University, Nanjing 210023, China

^cDepartment of Ultrasound, The Fourth Affiliated Hospital of Nanjing Medical University, Nanjing 210000, China

^dDepartment of Basic Medicine, Wuxi School of Medicine, Jiangnan University, Wuxi 214122, China

^eZhejiang Huafon New Materials Co., Ltd, Wenzhou 325200, China

Corresponding authors: Yao Liu (liuyao@njmu.edu.cn); Qingbo Lu (bonnielqb@yeah.net); Zhengdong Fei (zhengdongfei1982@163.com)



Figure S1 Imitation skin puncture model made of silicone.

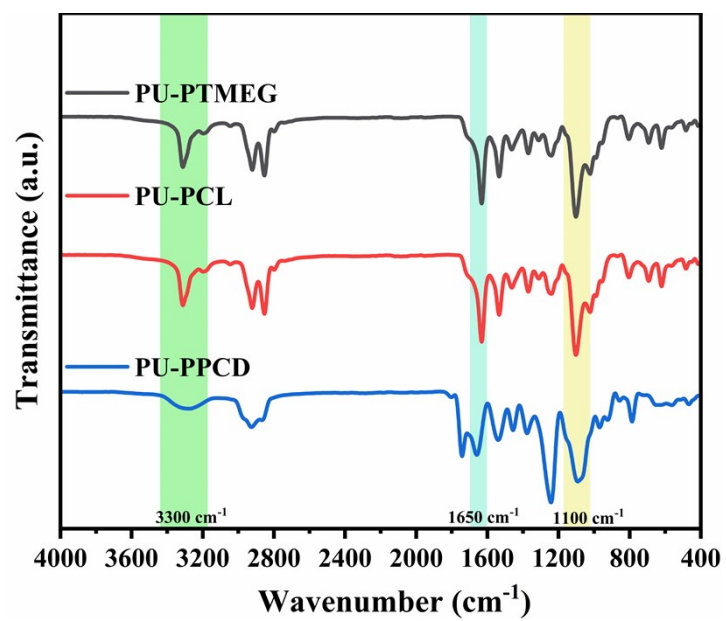


Figure S2 FTIR spectra of three TPUs in the range of 4000-400 cm⁻¹.

Molecular dynamics (MD) simulation

Cohesive energy density calculation. In the MD simulation, three TPU chains (PU-PTMEG, PU-PCL, and PU-PPCD) were constructed according to the chemical composition. Then, ten TPU chains with 100 repeat units were packed into the amorphous cell with three-dimensional periodic boundary conditions. The amorphous cell was geometrically optimized to minimize its potential energies. The energy convergence tolerance was set to 1.0×10^{-4} kcal mol⁻¹, the force convergence tolerance was 5.0×10^{-3} kcal mol⁻¹ Å⁻¹, the displacement tolerance was 5.0×10^{-5} Å, and the maximum optimization step was set to 500000. Then, the annealing operation was carried out, in which the starting temperature was 300 K, heating up to 500 K, and then cooling to 300 K. The above procedure was repeated five times. Then 1 ns of NVT (constant particle number, volume, and temperature of 298 K) and 1 ns of NPT (constant particle number, pressure of 1.0×10^{-4} GPa, and temperature of 298 K) simulations were performed. The resultant cells were used to calculate the cohesive energy density (CED).

Stress-strain behavior of PU-PTMEG. The resultant cells of PU-PTMEG after 1 ns of NPT simulation were subjected to a quasi-static stretching simulation with NVT ensemble at 298 K, and the strain at each stretch was set to 5%. Finally, the stress-strain curve of PU-PTMEG was obtained. The binding energy of the soft and hard segments ($E_{\text{hard/soft}}$) during the stretching process by

$$E_{\text{hard/soft}} = E_{\text{total}} - E_{\text{hard}} - E_{\text{soft}} \quad (\text{S1})$$

where E_{total} is the total energy of PU-PTMEG, E_{hard} is the total energy of hard segments, and E_{soft} is the total energy of soft segments.

Hydrogen bonds calculation. A hydrogen bond between two atoms will be created if the following criteria are met: (1) One atom is a hydrogen atom. The hydrogen atom is bound with a single bond and the attached atom may act as a hydrogen bond donor; (2) The second atom may act as a hydrogen bond acceptor and has at least one lone electron pair; (3) The distance between the hydrogen atom and the acceptor is less than or equal to the maximum hydrogen-acceptor distance (the maximum distance is set to 2.5 Å); (4) The value of the angle formed by the donor, hydrogen and acceptor atoms is at least

the minimum donor – hydrogen – acceptor angle (the minimum angle is set to 90°);
 (5) If both the hydrogen and acceptor atoms are within the same molecule, they are separated by at least four nearest neighbor shells.

In all the simulations, the Berendsen method was used to control pressure, and the Nose method was used to control temperature. The Verlet velocity–time integration method with a dynamic timestep of 1 fs was employed to integrate the Newtonian equation of motion. The Ewald method was used to calculate the electrostatic interactions with an accuracy of 1.0×10^{-4} kcal mol⁻¹ and a buffer width of 0.5 Å. The atom-based method was used to calculate the van der Waals interactions with a cutoff radius of 12.5 Å. All modeling and simulations are performed using Materials Studio software with the Condensed-Phase Optimized Molecular Potentials for Atomistic Simulation Studies (COMPASS) force field.

Density functional theory (DFT) calculations

The DFT calculations were executed using DMol3 code in the framework of the general gradient approximation (GGA) within the Perdew-Burke-Ernzerhof (PBE) exchange correlation functional. The double numerical plus polarization (DNP) was utilized as the numerical basis set during the simulation. The core electrons treatment was implemented by DFT semicore pseudopotential. The Monkhorst-Pack grid of $2 \times 2 \times 1$ k-point was used. A Fermi smearing of 0.005 Ha and a global orbital cutoff of 3.7 Å were set. The geometric optimizations were performed with a self-consistent field convergence tolerance of 10^{-6} Ha/atom, energy convergence tolerance of 10^{-5} Ha, maximum force convergence tolerance of 0.002 Ha/Å, and maximum displacement convergence tolerance of 0.005 Å. The binding energies (E_{binding}) between hard segment dimer were calculated using DMol3 code by the following equation:

$$E_B = E_{\text{com}} - \sum E_{\text{fra}} \quad (\text{S2})$$

where E_{com} is the total energy of the hard segment dimer, E_{fra} is the energy of each hard segment.

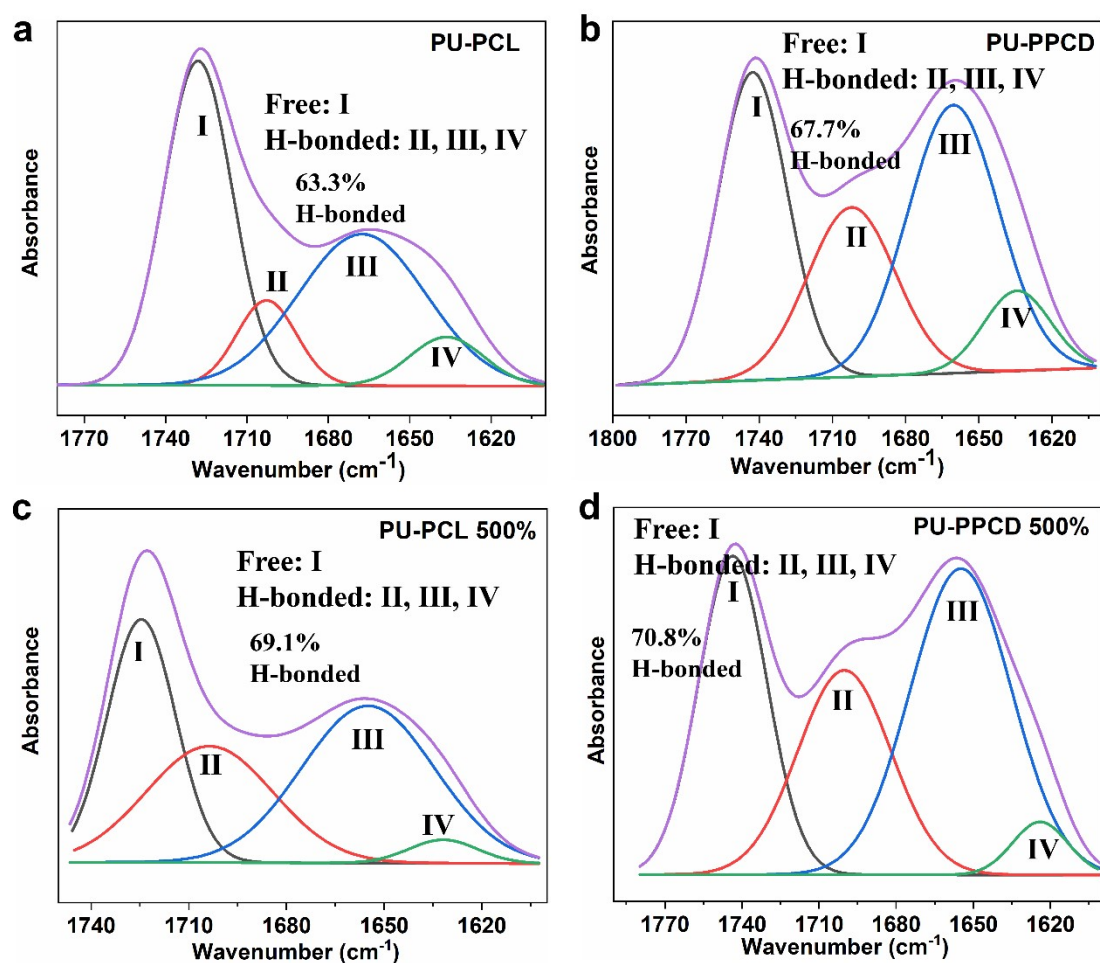


Figure S3 FTIR spectra of (a) PU-PCL and (b) PU-PPCD are deconvoluted in the carbonyl region at 0 strain. FTIR spectra of (c) PU-PCL and (d) PU-PPCD are deconvoluted in the carbonyl region at 500% strain.

The detailed calculation method for \bar{M}_c

The σ_t versus (λ^2-1/λ) curves are obtained by σ_t versus strain (ε) curves. $\lambda=l/l_0$ is defined as the elongation ratio, and thus $\varepsilon = l/l_0 - 1 = \lambda - 1$. l and l_0 represent the length of the sample after drawn and gauge length, respectively. The σ_t versus (λ^2-1/λ) curve can be fitted with $\sigma_t = Y + G_p (\lambda^2-1/\lambda)$, where Y relates to the extrapolated yield stress and G_p is defined as the strain hardening modulus. G_p can be further expressed as a function of $\rho RT / \bar{M}_c$, where the density of materials, ρ (g/cm³), is measured to be ~ 1.1 g/cm³, R (J mol⁻¹ K⁻¹) is the ideal gas constant, T (K) is the absolute temperature and \bar{M}_c (g/mol) is the average constraint molecular weight between the physical crosslinking junctions.

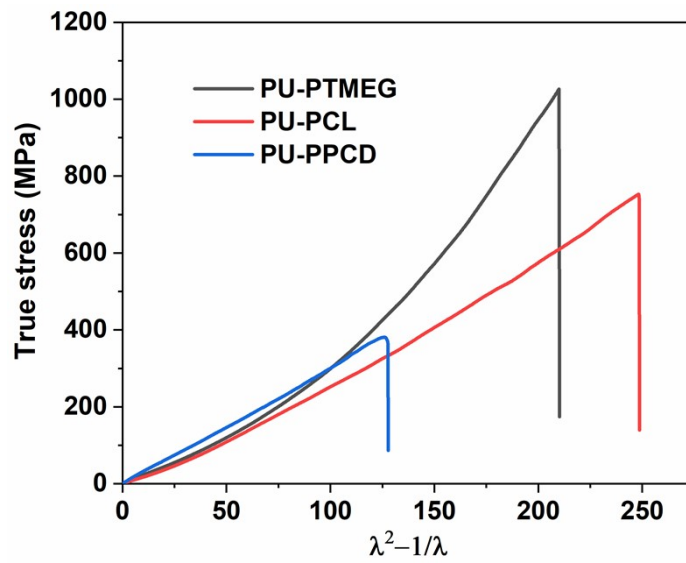


Figure S4 σ_t versus (λ^2-1/λ) curves of PU-PTMEG, PU-PCL, and PU-PPCD elastomers.

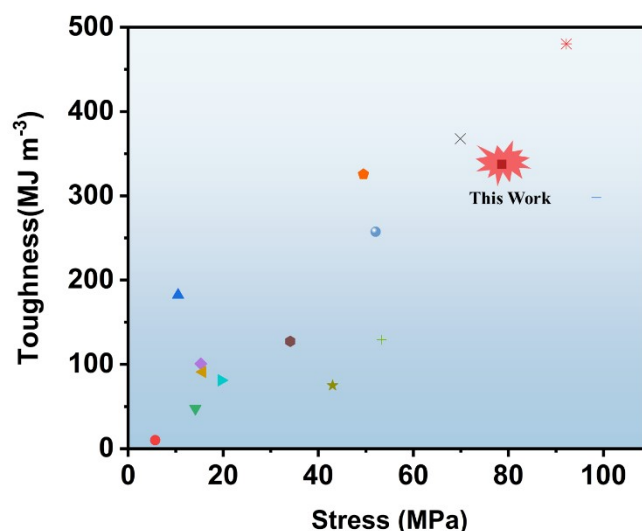


Figure S5 Comparative Chart of Material Mechanical Properties

Molecular Modeling and Interaction Energy Analysis of TPU Soft-Segment Dimers

To quantitatively assess the intermolecular interactions of different soft segments, two-chain (dimer) models of PTMEG, PCL, and PPCD were constructed using Materials Studio 2020. Each model consisted of two identical oligomer chains (molecular weight $\approx 2000 \text{ g mol}^{-1}$) placed in close proximity within a periodic simulation box. Geometry optimizations were performed using the Forcite module with the COMPASS II force field until the energy convergence reached $1.0 \times 10^{-4} \text{ kcal mol}^{-1}$.

The binding energy (E_{binding}) between the two chains was calculated as:

$$E_{\text{binding}} = E_{\text{total}} - 2E_{\text{single}}$$

where E_{total} is the total potential energy of the two-chain system and E_{single} is the energy of an isolated single chain. A more negative E_{binding} indicates stronger intermolecular interactions.

The calculated binding energies were $-36.02 \text{ kcal mol}^{-1}$ for PTMEG, $-58.16 \text{ kcal mol}^{-1}$ for PCL, and $-70.87 \text{ kcal mol}^{-1}$ for PPCD, indicating that the intermolecular interaction strength follows the order $\text{PTMEG} < \text{PCL} < \text{PPCD}$ (in absolute value).

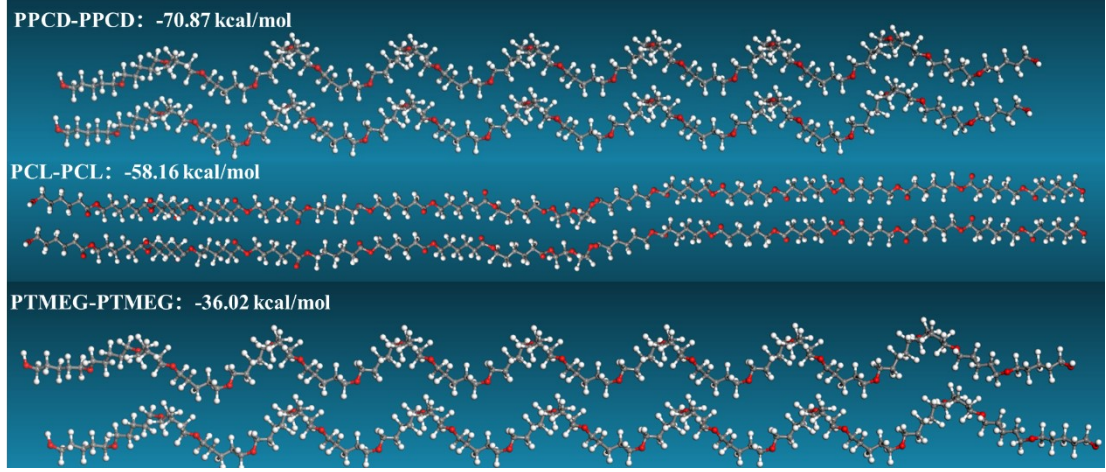


Figure S6 Energy map for soft dimer interactions

Calculation details for the true stress-strain

True stress-strain curves are derived from the engineering stress-strain curves by the following equations:

$$\sigma_t = \sigma \frac{l_0 + \Delta l}{l_0} = \sigma(1 + \varepsilon) \quad (\text{S3})$$

$$\varepsilon_t = \int_{l_0}^{l_f} \frac{dl}{l} = \ln \frac{l_f}{l_0} = \ln(1 + \varepsilon) \quad (\text{S4})$$

Where σ_t is the true stress, σ is the engineering stress, l_0 is the original length of the specimen, l is the instant length of the deformed specimen, $l_f = l_0 + \Delta l$ is final length of the fractured specimen, ε_t is the true strain, and ε is the engineering strain.

Fracture energy test

The fracture energy test was conducted by the tensile test using the single-edge notched sample. The notched and unnotched samples (gauge length of 20 mm, width

of 4 mm, thickness of 1.0 mm) were both tested with a strain speed of 3 mm min⁻¹. The fracture energy (G_c) was calculated by

$$G_c = \frac{6wc}{\sqrt{\lambda_c}} \quad (S5)$$

where c is the length of the slit (1 mm), λ_c is the elongation ratio-at-break of the notched sample, w is the strain energy calculated by integration of the stress-strain curve of the unnotched samples. The elongation-at-break $\varepsilon_c = \lambda_c - 1$.

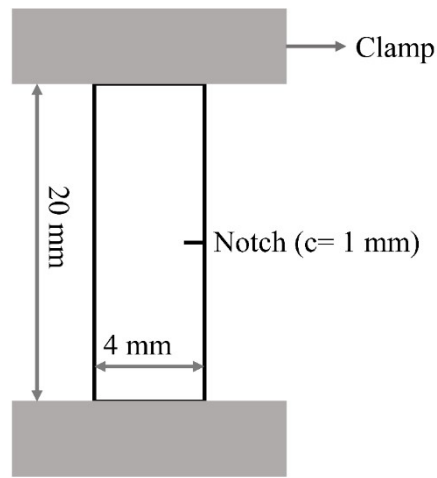


Figure S7 Dimensions of the notched tensile sample.

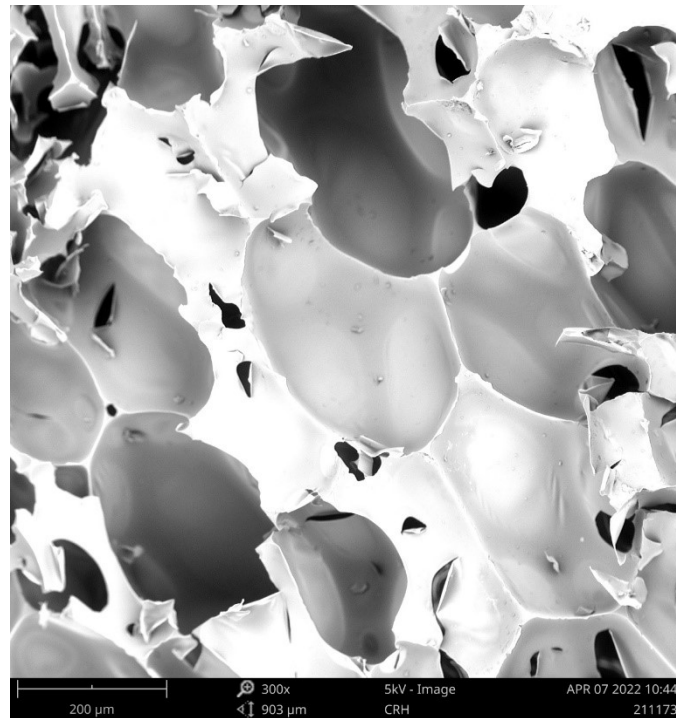


Figure S8 Scanning electron microscope image of commercialized rigid polyurethane foam.

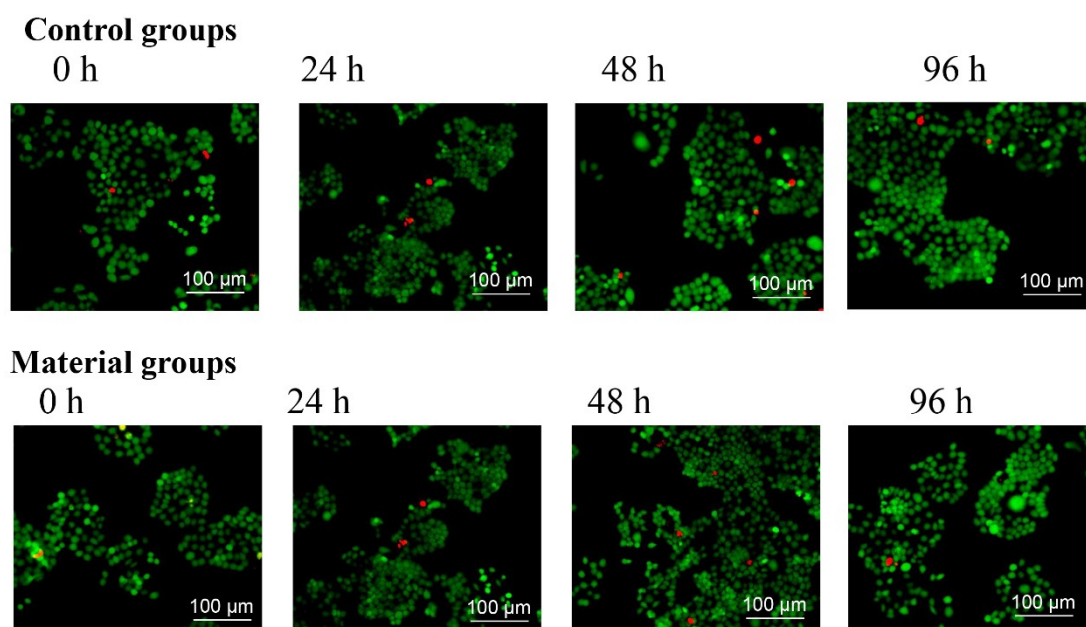


Figure S9 Cell viability test at 5 mg/ml for different times.

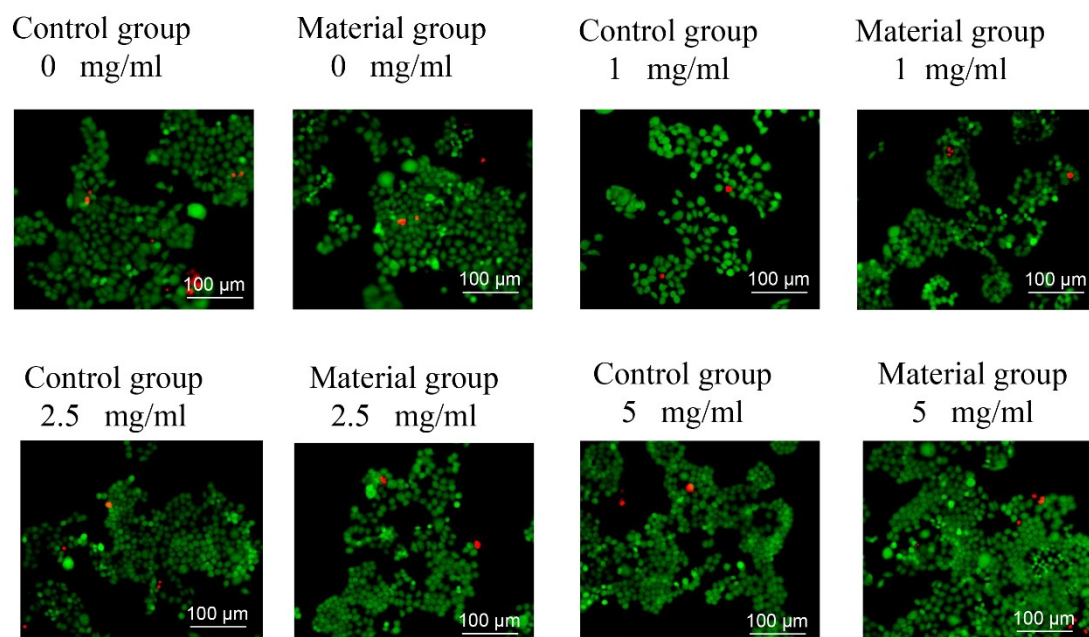


Figure S10 24-hour cell viability test at different TPU concentrations.

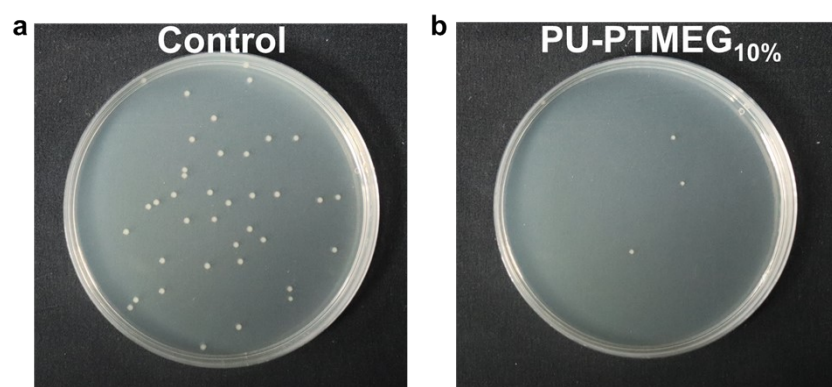


Figure S11 Photographs of *E. coli* colonies in different culture media. The control group consists of media without PU-PTMEG fibers.

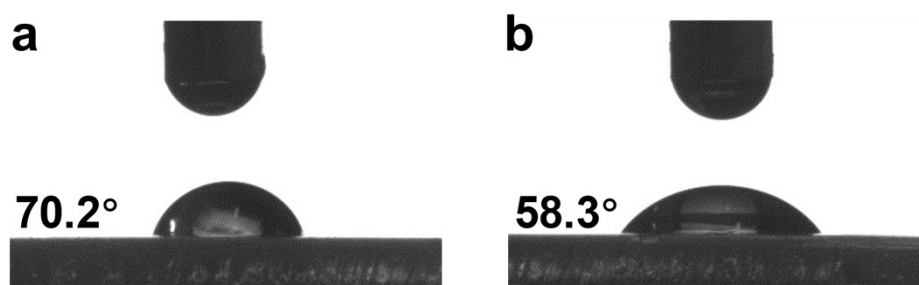


Figure S12 (a) shows the contact angle measurement result of PU-PTMEG without hydrazide groups. (b) presents the result of the sample containing hydrazide groups with the same PU-PTMEG formulation.

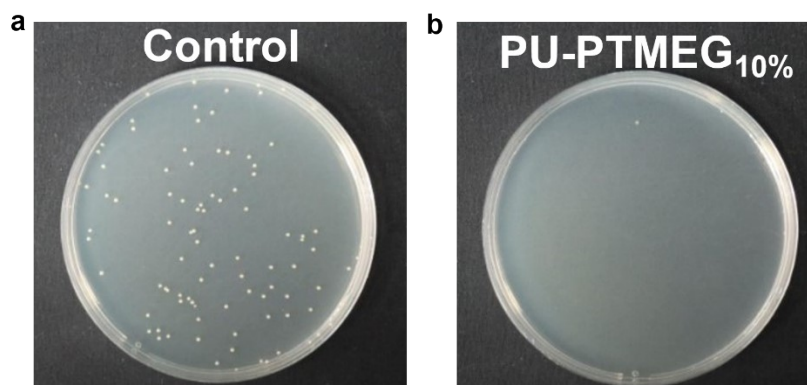


Figure S13 The cell morphology and adhesion quantity: (a) PU-PTMEG without SPH Bacterial adhesion: 9.3×10^6 CFU/disc; (b) PU-PTMEG10% Bacterial adhesion: 1.5×10^4 CFU/disc.

Table S1 GPC results of TPU

Samples	M_n (g mol ⁻¹)	M_w (g mol ⁻¹)	PDI
PU-PTMEG	54100	107400	1.98
PU-PCL	54300	112700	2.08
PU-PTMEG	59000	112900	1.91

Table S2 Hydrogen bonding structures of PU-PTMEG, PU-PCL, and PU-PPCD at 0 strain

Assignment		Wavenumber (cm ⁻¹)			Area (%)		
		PU-PTMEG	PU-PCL	PU-PPCD	PU-PTMEG	PU-PCL	PU-PPCD
ν (C=O)	Free (I)	1710	1727	1742	17.7	36.7	32.3
ν (C=O in urethane group)	Disordered (II)	1663	1703	1702	31.3	28.9	22.8
	Ordered (III)	1634	1658	1660	41.0	25.8	33.8
ν (C=O in urea groups)	Ordered (IV)	1616	1636	1634	10.0	8.6	11.1
H-bond content					82.3	63.3	67.7

Table S3 Hydrogen bonding structures of PU-PTMEG, PU-PCL, and PU-PPCD at 500% strain

Assignment		Wavenumber (cm ⁻¹)			Area (%)		
		PU-PTMEG	PU-PCL	PU-PPCD	PU-PTMEG	PU-PCL	PU-PPCD
ν (C=O)	Free (I)	1710	1724	1743	26.9	30.9	29.2
ν (C=O in urethane group)	Disordered (II)	1691	1703	1700	7.3	27.4	25.5
	Ordered (III)	1657	1654	1654	58.9	35.2	34.4
ν (C=O in urea groups)	Ordered (IV)	1629	1631	1623	6.9	6.5	10.9
H-bond content					73.1	69.1	70.8

Table S4 Comparison of mechanical properties of representative TPUs reported in literature

Materials	Stress (MPa)	Toughness (MJ m ⁻³)	Refs.
PU-PTMEG	78.6	337.4	This work
PFBC	5.7	10.1	29
SPUE	10.5	182.2	32
WPU-IPDA-Zn	14.15	47.57	34
WTA-4	15.3	100.75	32
WPU8	15.67	91	33
PSUA-3	19.6	81	34
SPU	34.1	127.3	35

C-IP-SS	43	75	36
SPUU-3	49.52	325.54	41
SWPU-DESH-Zn	52.07	257.40	37
WPU-UPy-3	53.33	128.97	38
PCL-IPDI-BHO	92.2	480.2	39
PU-OD	98.5	298	40